



**AUIQ Complementary Biological System**

ISSN: 3007-973X

Journal homepage:

<https://acbs.alayen.edu.iq>



Volume 1 | Issue 1

Article 1

## Conversion of Chicken Rice Waste into Char via Hydrothermal, Pyrolysis, and Microwave Carbonization Processes: A Comparative Study

Mahmod A. Abdulqader

*Oil Products Distribution Company, (OPDC) Salahuldeen Branch, Tikrit, Ministry of Oil, Iraq*

Muhammad Akromin Suliman

*Faculty of Applied Sciences, Universiti Teknologi MARA, 40450 Shah Alam, Selangor, Malaysia*

Tabit Abas Ahmed

*Directorate of Training and Development, Ministry of Oil, Iraq*

Ruihong Wu

*Department of Chemistry, Hengshui University, 053500, Hebei Province, Hengshui, China*

Aiman. M. Bobaker

*Chemistry Department, Faculty of Science, University of Benghazi, Benghazi, Libya*

Tiyasha Tiyasha

*Department of Civil Engineering, School of Engineering and Computing, Dev Bhoomi Uttarakhand University, Dehradun, India*

Mohamed A. Yassin

*Interdisciplinary Research Center for Membranes and Water Security, KFUPM, 31261, Saudi Arabia*

Nabil Al-Areeq

*Department of Geology and Environment, Thamar University, Thamar, Yemen*

Follow this and additional works at: <https://acbs.alayen.edu.iq/journal>



Part of the Life Sciences Commons

### Recommended Citation

Abdulqader, Mahmod A.; Suliman, Muhammad Akromin; Ahmed, Tabit Abas; Wu, Ruihong; Bobaker, Aiman. M.; Tiyasha, Tiyasha; Yassin, Mohamed A.; and Al-Areeq, Nabil (2024), Conversion of Chicken Rice Waste into Char via Hydrothermal, Pyrolysis, and Microwave Carbonization Processes: A Comparative Study, *AUIQ Complementary Biological System*: Vol. 1: Iss. 1, 1-9.

DOI: <https://doi.org/10.70176/3007-973X.1003>

Available at: <https://acbs.alayen.edu.iq/journal/vol1/iss1/1>



ORIGINAL STUDY

# Conversion of Chicken Rice Waste into Char via Hydrothermal, Pyrolysis, and Microwave Carbonization Processes: A Comparative Study

Mahmod A. Abdulqader<sup>a,\*</sup>, Muhammad Akromin Suliman<sup>b</sup>, Tabit Abas Ahmed<sup>c</sup>, Ruihong Wu<sup>d</sup>, Aiman. M. Bobaker<sup>e</sup>, Tiyasha Tiyasha<sup>f</sup>, Mohamed A. Yassin<sup>g</sup>, Nabil Al-Areeq<sup>h</sup>

<sup>a</sup> Oil Products Distribution Company, (OPDC) Salahuldeen Branch, Tikrit, Ministry of Oil, Iraq

<sup>b</sup> Faculty of Applied Sciences, Universiti Teknologi MARA, 40450 Shah Alam, Selangor, Malaysia

<sup>c</sup> Directorate of Training and Development, Ministry of Oil, Iraq

<sup>d</sup> Department of Chemistry, Hengshui University, 053500, Hebei Province, Hengshui, China

<sup>e</sup> Chemistry Department, Faculty of Science, University of Benghazi, Benghazi, Libya

<sup>f</sup> Department of Civil Engineering, School of Engineering and Computing, Dev Bhoomi Uttarakhand University, Dehradun, India

<sup>g</sup> Interdisciplinary Research Center for Membranes and Water Security, KFUPM, 31261, Saudi Arabia

<sup>h</sup> Department of Geology and Environment, Tamar University, Tamar, Yemen

## ABSTRACT

This study aims to convert chicken rice waste (CRW) to chars by hydrothermal carbonatization (HTC), pyrolysis (PY), and microwave irradiation (MW) processes. The operating parameters affecting the HTC process (range of temperatures 120, 140, 160, 180, and 200 °C) for hydro-char production, while the pyrolysis (range of temperatures 400, 500, 600, and 700 °C) for pyro-char production, and microwave irradiation (range of microwave power 200, 400, 600, and 800 W) for micro-char production were investigated. Comparative studies of the physicochemical properties of produced chars were investigated by Brunauer-Emmett-Teller (BET), X-ray diffraction (XRD), Fourier transform infrared (FTIR), and scanning electron microscope (SEM). The results showed that the hydro-char produced by the HTC process at a temperature of 200 °C achieved the optimal solid yield (62.5 %), while the pyro-char produced by the PY process at a temperature of 700 °C achieved the optimal solid yield (37.18 %), and the micro-char produced via microwave irradiation process at a microwave power of 800 W achieved the optimal solid yield (37.18 %). The BET surface area of CRW, HTC200, PY700, and MW800 are 0.19 m<sup>2</sup>/g, 1.22 m<sup>2</sup>/g, 68.98 m<sup>2</sup>/g, and 0.19 m<sup>2</sup>/g, respectively. The results of the current study clarified that the chars produced from CRW during HTC, PY, and MW techniques could be used for energy production and wastewater treatment. As well as recommendations, this study needs to be sustained by doing some descriptions such as high heating value (HHV).

**Keywords:** Chicken rice waste, Hydro-char, Pyro-char, Micro-char, Solid carbon

## 1. Introduction

According to the World Bank, global food waste (FW) is anticipated to climb by up to 70 % by 2050, coinciding with a 29 % population increase. Food that has not served its intended function is deemed

food waste (FW) (US EPA, 2022) [1]. Global FW is growing alongside population and food consumption [2]. Globally, 17 billion tons of trash are generated each year as a result of growing industry and urbanization; by 2050, this figure will rise to 27 billion [3]. Rice waste can be utilized as a raw material

Received 30 April 2024; accepted 28 May 2024.  
Available online 29 June 2024

\* Corresponding author.  
E-mail address: mahmodabdulkarem1978@gmail.com (M. A. Abdulqader).

<https://doi.org/10.70176/3007-973X.1003>

3007-973X/© 2024 Al-Ayen Iraqi University. This is an open access article under the CC BY-NC-ND license (<http://creativecommons.org/licenses/by-nc-nd/4.0/>).

in agriculture for a variety of purposes, including increasing soil fertility through carbonization and composting, generating renewable energy, and producing industrial-grade silica and biofiber. These are only some of the numerous possible benefits of employing rice waste in agriculture [4]. As the scale of chicken production increases, so does the amount of manure produced. Chicken manure is regarded as a good soil amendment due to its high nitrogen and phosphorus content. However, the large production of manure surpasses the soil's needs. Rice trash is a byproduct of rice production [5].

As a result, efficient discarding, energy yield, and conversion into vital materials of food waste have attracted significant attention [6]. The conversion of food waste into char is regarded as the optimum yield compared to disposal and energy yield, where the disposal of food waste needs a high cost and can cause damage to natural resources [7]. Consequently, thermochemical conversion processes (e.g., hydrothermal carbonization, pyrolysis, and microwave irradiation) could be used for the conversion of food waste to chars with enhanced energy properties [8]. Because of its exceptional physicochemical properties, the resulting carbonaceous material (char or activated carbon) can be employed as a solid carbon fuel and adsorbent in combustion plants and wastewater treatment systems. Chars are a type of carbonaceous substance that can be created through the thermal treatment of food waste [9]. Chars exhibit distinct physiochemical features, including as enriched surface functional groups, high pore volume, high specific surface area, mesoporous structure, high carbon dioxide fixation efficiency, high mineral content, high calorific value, and thermal stability [10]. Char has received a lot of attention for its remarkable qualities in a variety of applications [11], including soil remediation [12], composting additives [13], pollutant removal from wastewater [14], greenhouse gas emissions reduction [15], catalysts [16], and the energy industry [17].

In this work, the chicken rice waste is chemically degraded via thermochemical ways, with the hydrothermal carbonization process due to various temperatures from 120 to 200 °C to hydro-char production, while the pyrolysis process including the anaerobic decomposition of chicken rice waste at temperatures ranging from 400 to 700 °C to generate an alternative fuel (pyro-char), and the micro-char produced during the microwave irradiation relating the utilization of microwave irradiation at power range from 200 to 800 W. In the same context, in the HTC process, the water may play a major role by covering the raw material, which facilitates the process of thermochemical conversion and the occurrence of

dehydration and decarboxylation processes [18]. Via the pyrolysis conversion process, energy from the power supply is converted into heat, which is then transferred to the target material surface and, finally, the inner parts via convection and conduction. As a result, heating performance is frequently limited by surface temperature and thermophysical properties of the chosen material, such as heat capacity, density, and thermal conductivity [19]. On the contrary, the microwave irradiation technique generates heat through the microwave irradiation interaction with the dipoles of the chosen material, resulting in even heat distribution, controllability, and great heating precision. The heating methods used in the two thermochemical processes are expected to have a major impact on the physical and chemical properties of the final materials [20].

Thus, this study aims to apply three thermochemical technologies including hydrothermal carbonization, pyrolysis, and microwave to convert the chicken rice waste into value-added products such as hydro-char obtained by hydrothermal carbonization, pyro-char obtained by pyrolysis and micro-char obtained by microwave. Comparative studies for the physicochemical characteristics of CRW, hydro-char, pyro-char, and micro-char were achieved by several instruments like Brunauer Emmet Teller (BET), Fourier transform infrared (FTIR) spectroscopy, X-ray diffraction (XRD), thermogravimetric and derivative thermogravimetric (TGA), and scanning electron microscopy (SEM). The suitability of hydro-char, pyro-char, and micro-char as solid carbon fuels was investigated by analyzing their energy characteristics, for example, solid yield product, optimal reaction temperature for hydrothermal carbonization, pyrolysis, and optimal microwave power for the microwave irradiation process.

## 2. Materials and methods

### 2.1. Materials

The chicken rice waste (CRW) was collected from a Chicken rice stall at a café in the Faculty of Applied Science Universiti Teknologi Mara campus in Shah Alam, Selangor, Malaysia. Then, CRW was washed with tap water to remove other waste such as soy sauce and vegetable waste. The CRW was dried in the oven at 90 °C, for 24 h before crushing and grinding. Next, it was sieved to a certain particle size  $\leq 250 \mu\text{m}$ . Raw material from CRW comprised 50% rice, 25% bones, and 25% meats prepared by weight percentage (%) by mixing the chicken rice waste and drying it in an oven for 24 h at 90 °C. Before additional studies, three (3) portions each of 10 g of the mixed samples

(1 mm size) were measured and stored in a desiccator in a plastic bag. Then, subjected it to (HTC), (PY), and (MW) techniques were subjected to the thermochemical conversion of each sample into hydro-char, pyro-char, and micro-char respectively.

## 2.2. Preparation of chars

Fig. 1 shows the hydro-char, pyro-char, and micro-char were prepared via HTC, PY, and MW processes respectively. The hydro-char produced via the HTC process of 10 g of CRW was thoroughly mixed with 100 mL (1:10) solid-to-liquid in distilled water before being transferred to an automated stainless steel hydrothermal reactor (170 mL) autoclave. After 30 minutes of stirring, the temperature was raised from room temperature at a rate of 5 °C/min until it

reached 120 °C, and had been kept there for 180 min, with N<sub>2</sub> pressure at 4 MPa (closed system). The reactor was gradually cooled to room temperature at the end of the reaction time. The hydro-char particles were then vacuum filtered out of the reaction mixture and washed several times with hot distilled water. The samples were dried in an oven at 90 °C for 24 hours. The hydrothermally carbonized sample was stored in a small plastic container marked HTC 120. This procedure was repeated at temperatures of 140, 160, 180, and 200 °C to produce HTC140, HTC160, HTC180, and HTC220, respectively.

While the pyro-char was prepared via the PY process 10 g of CRW was placed in a tubular GSL-1100X quartz furnace with a programmable temperature controller (0.025 ≈ 0.051 m diameter). The N<sub>2</sub> gas (99.99%) was delivered to the furnace at a rate of

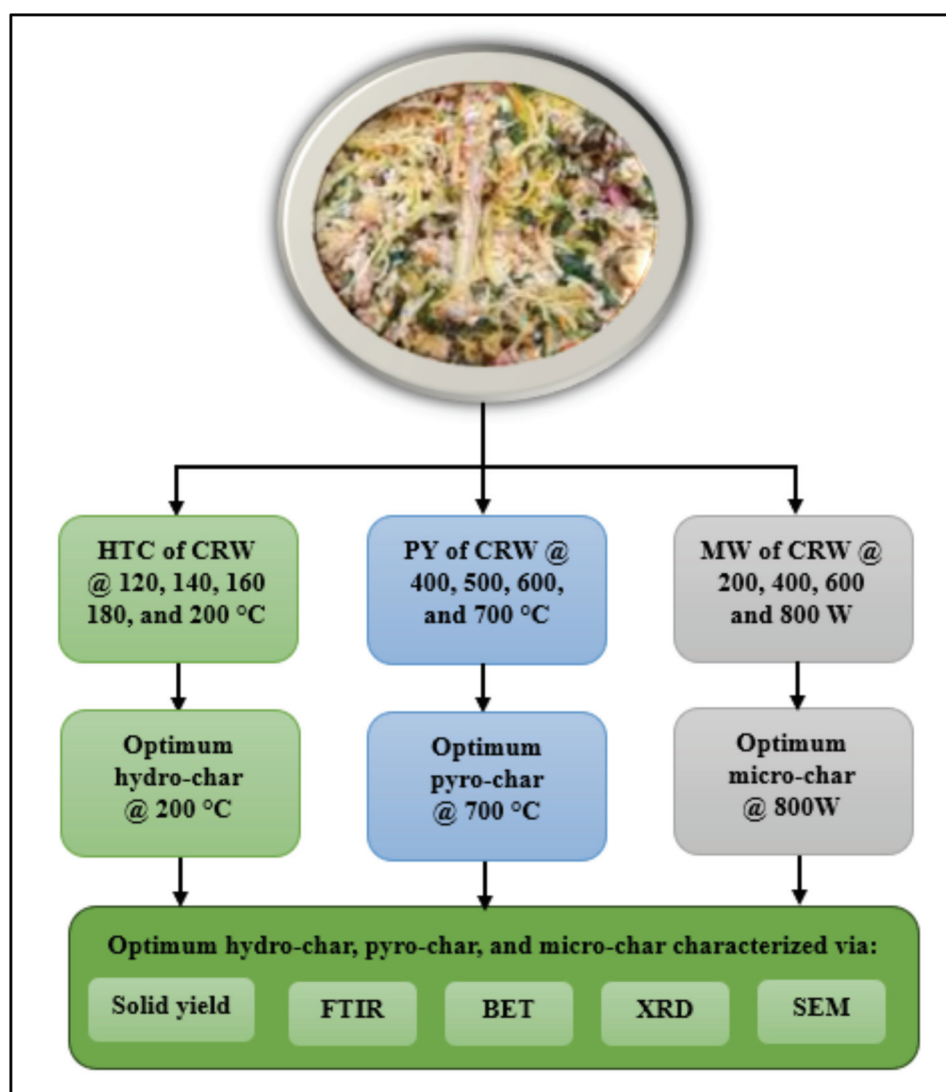


Fig. 1. Schematic diagram for HTC, PY, and MW processes.

2L/min. During the first experimental run, the furnace temperature was raised from room temperature to 500 °C. The sample was kept at this temperature for 60 min inside the furnace before being rapidly cooled to room temperature using N<sub>2</sub> gas flow. The pyrolyzed char produced was stored in a small plastic container labeled PY500. The other sample runs were also carried out at 600, 700, and 800 °C, with the sample chars produced labeled PY600, PY700, and PY800, respectively.

Finally, the micro-char produced by the MW process 10 g of CRW was placed in a quartz cell before being transferred to a modified microwave oven (Samsung ME711K, 20 L). The sample was microwave-irradiated at 200 W for 10 minutes while being fed a 2 L/min flow of pure N<sub>2</sub> pressure (99.99 percent) gas. The microwave sample was allowed to cool to ambient temperature inside the reactor under N<sub>2</sub> gas flow before being packaged in a plastic sample container labeled MW200. The sample runs were carried out in the same MW manner, but the microwave irradiation power was increased to 400W, 600W, and 800W, respectively, to obtain MW400, MW600, and MW800 samples.

### 2.3. The physicochemical properties of CRW and optimized chars

The solid yield chars product was calculated depending on Equation (1). The textile properties (e.g., surface area and mean pore diameter) of CRW, HTC200, PY700, and MW800 were determined via (Micromeritics ASAP 2020 analyzer). The amorphous nature and crystallinity of CRW, HTC200, PY700, and MW800 were characterized using an instrument X-ray diffractometer (XRD, Rigaku Ultima IV). The functional groups of CRW, HTC200, PY700, and MW800 were identified by Fourier transform infrared spectrophotometer (FTIR, Perkin-Elmer, Spectrum RX I). The morphological characteristics of CRW, HTC200, PY700, and MW800 were obtained by scanning electron microscopy (SEM, model SU3500, Hitachi).

$$\text{Char yield, \%} = \frac{\text{weight}_{\text{char}}}{\text{weight}_{\text{CRW}}} \times 100 \quad (1)$$

## 3. Results and discussion

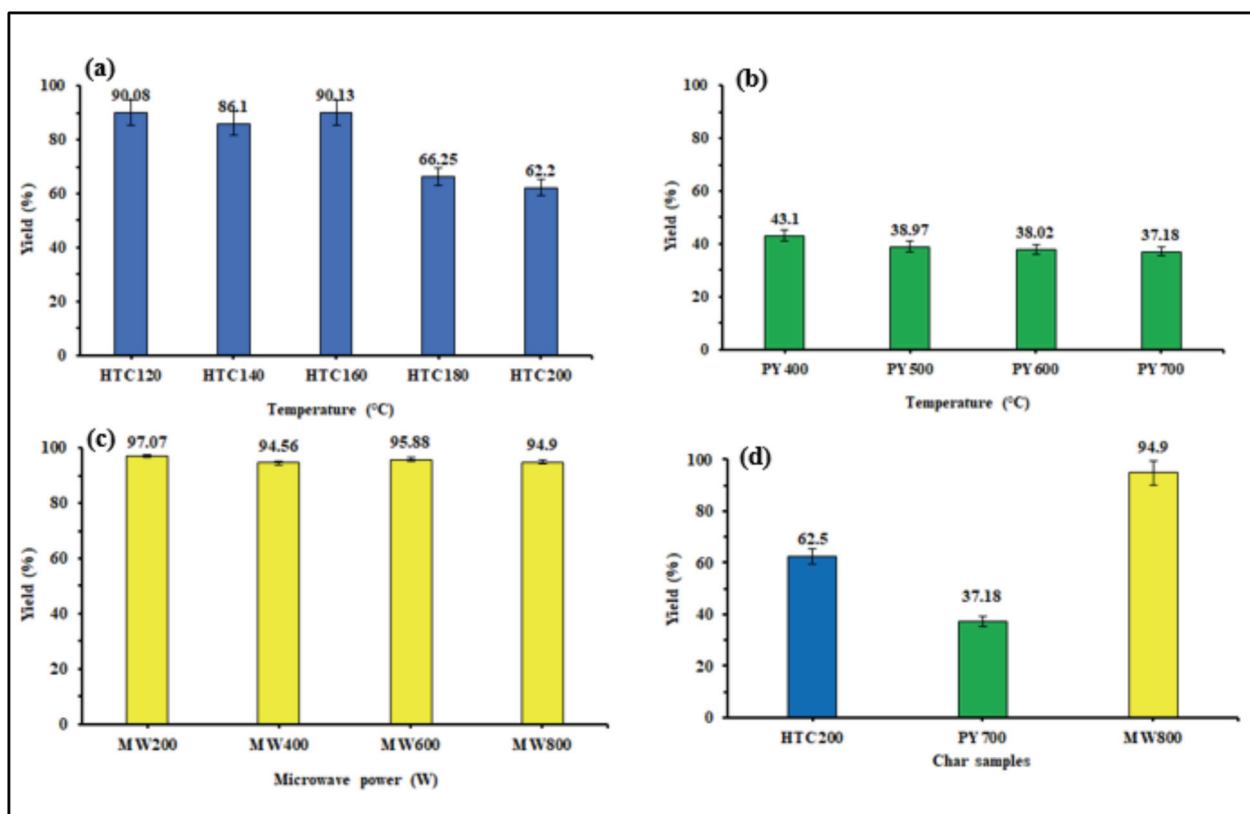
### 3.1. Chars yield percentage

Fig. 2 shows the solid yield produced through the HTC, PY, and MW processes. As the hydrothermal

temperature climbed from 120 to 200 °C, the mass yield of the hydro-char decreased (90.08 to 62.20 %) [21]. Following pyrolysis, the mass yield of the pyro-char decreased (43.10 to 37.18 %) from 400 to 700 °C [22], and microwave irradiation process the mass yield of the micro-char decreased (97.07 to 94.90 %) of the CRW combination from 200 to 800 W, a similar declining trend in solid yield was observed which indicates the effectiveness of the thermochemical conversion processes [23]. The reaction temperature negatively affects the solid yield in thermochemical conversion, as well as power in the microwave process. In other words, the higher the reaction temperature, the lower the solid yield [24]. Moreover, in this study, the thermochemical conversion processes focused on the highest temperatures in HTC, and PY while on the highest microwave power in the MW. For this reason, it was taken into consideration that the lower the solid yield due to the effect of temperature, and microwave power, the greater the efficiency of the product, then the characterization was carried out to the highest temperatures and microwave power. As a result, optimal hydro-char was found HTC200 during the HTC, while optimal pyro-char was found PY700 during the PY, and finally optimal micro-char during MW irradiation of CRW processes [25].

### 3.2. FTIR spectral analysis

Proof of identity of the functional groups in the prepared structures CRW, HTC200, PY700, and MW800 utilized by FTIR test. Fig. 3 shows FTIR spectra of (a) CRW, (b) HTC200, (c) PY700, and (d) MW800, respectively. The absorption wavelengths in the 3500–3800 cm<sup>-1</sup> range for CRW, HTC200, PY700, and MW800 are credited to the stretching vibration mode of amine (N–H) groups from phenolic, alcoholic, and nitrogenous compounds [26]. The peaks concentrated in the range of 2400 cm<sup>-1</sup> in the spectrum are related to the alkanes stretching of the C–H bond in aliphatic compounds [27]. The disappearance of this peak in the spectrum (see Fig. 4) indicated the lowering of the aliphatic content in CRW, HTC200, PY700, and MW800. The peak located at 3000 cm<sup>-1</sup> in the spectrum of HTC200, PY700, and MW800 is correlated to (C=H) stretching, while the peaks located at 1400 cm<sup>-1</sup> in CRW, HTC200, PY700, and MW800 are linked with carbonyl bond (C=O) [6]. The small bands demonstrated at 1000 cm<sup>-1</sup> in the spectra of HTC200, PY700, and MW800 may be ascribed to the stretching vibration of C–C in aromatic compounds [28].



**Fig. 2.** Chars yield percentage (a) hydro-char produced via HTC process at various temperatures, (b) pyro-char produced via PY process at various temperatures (c) micro-char produced via MW irradiation process at various microwave power (d) optimal hydro-char, pyro-char, micro-char.

### 3.3. Specific surface area (BET) test

The textural properties (like., BET surface area, Langmuir surface area, and mean pore diameter) of CRW, HTC200, PY700, and MW800 are shown in Table 1. The BET surface area of PY700 ( $68.98 \text{ m}^2/\text{g}$ ) was significantly greater than that of CRW ( $0.19 \text{ m}^2/\text{g}$ ), HTC200 ( $1.22 \text{ m}^2/\text{g}$ ), and MW800 ( $14.7 \text{ m}^2/\text{g}$ ), as detailed in Table 1. The improvement in the BET surface area for PY700 reached 530 times compared to CRW, 56 times compared to HTC200, and 4.8 times compared to MW800. This finding is related to the pyrolysis temperature, which has a substantial impact on the BET surface area of the PY700

**Table 1.** Textural properties of CRW, HTC200, PY700, and MW800.

Sample	BET surface area ( $\text{m}^2/\text{g}$ )	Langmuir surface area ( $\text{m}^2/\text{g}$ )	Mean pore diameter (nm)
CRW	0.13	ND	ND
HTC200	1.22	1.86	0.22
PY700	68.98	149.22	0.22
MW800	14.7	26.9	0.99

ND: Not detected.

due to the pyrolysis process's uniform distribution of temperature, controllability, and temperature accuracy [29]. Furthermore, the mean pore diameter of CRW, HTC200, PY700, and MW800 are not detected, 0.22 nm, 0.22 nm, and 0.99 nm, respectively. These findings reflected that the produced chars possess a microporous structure (mean pore diameter less than 2 nm) according to the IUPAC classification [30].

### 3.4. XRD analysis

The XRD analysis was utilized to obtain information about the nature of raw CRW structure and to describe the crystallinity of the chars produced for HTC200, PY700, and MW800. The XRD patterns of CRW, HTC200, PY700, and MW800 are illustrated in Fig. 4. As shown in Fig. 3(a), the XRD spectrum of CRW depicts various peaks, which are linked to inorganic materials presented in the raw material such as muscovite 2M2 ( $\text{K}_{0.77}\text{Al}_{1.93}(\text{Al}_{0.5}\text{Si}_{3.5})\text{O}_{10}(\text{OH})_2$ ), dolomite ( $\text{CaMg}(\text{CO}_3)_2$ ), calcite ( $\text{CaCO}_3$ ), barite ( $\text{BaSO}_4$ ), and quartz ( $\text{SiO}_2$ ) [31]. The XRD spectrum of HTC200 showed that the HTC200 possesses a

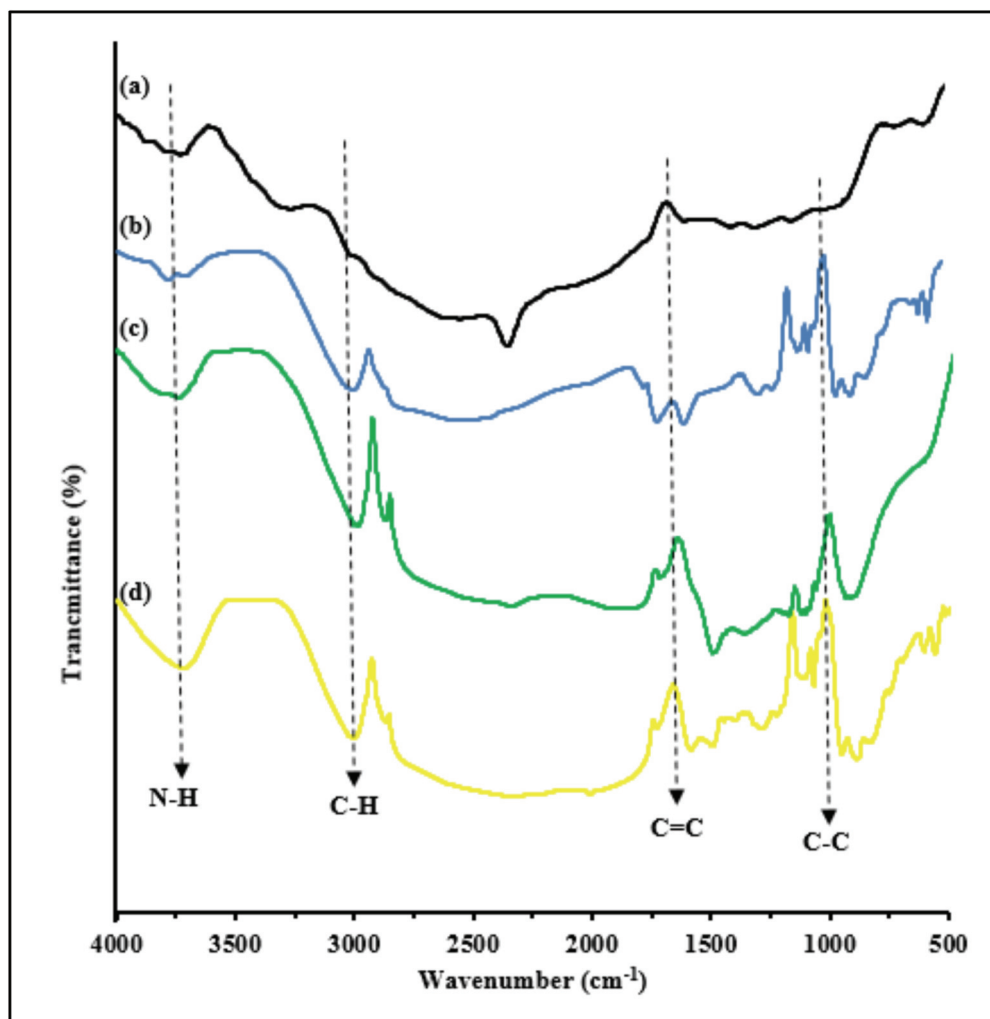


Fig. 3. FTIR spectra of (a) CRW, (b) HTC200, (c) PY700, and (d) MW800.

crystalline nature due to the presence of sharp peaks, which are connected with quartz and graphite materials. Regarding the XRD spectrum of PY700, MW800, the amorphous nature was deduced from the broad bands centered at  $24^\circ$  and  $44^\circ$ , which are ascribed to the crystallographic planes of carbonaceous compounds [32].

### 3.5. SEM analysis

SEM was utilized to inspect the surface morphology of CRW, HTC200, PY700, and MW800 as well as to compare the difference in pore surface structure of chars materials synthesized by HTC, PY, and MW approaches. Fig. 5 explains the SEM images of (a) CRW, (b) HTC200, (c) PY700, and (d) MW800 at high magnifications of  $\times 500$ . Fig. 4(a) shows the exterior surface of the raw CRW was reasonably smooth and had a relatively regular matrixed structure with a

noticeable absence of pores, suggesting that the CRW particles are evenly coated with protein [33]. The morphological structure of CRW, HTC200, PY700, and MW800 materials produced from hydrothermal carbonization, pyrolysis, and microwave ways, (see Fig. 4) respectively, appeared to be heterogeneous and amorphous structures containing the even distribution of pores in the structure along with the cracks and crevices. The presence of pores on the surface of HTC200, PY700, and MW800 can be ascribed to the carbonization process during the hydrothermal carbonization, pyrolysis, and microwave processes, causing the release of volatile compounds like hydrocarbons, hydrogen, and carbon dioxide from the raw CRW [34]. The generation of the porous structure of HTC200, PY700, and MW800 suggests that it can be employed in energy applications like dry methane reforming to attain clean fuels i.e. hydrogen and syngas [35].

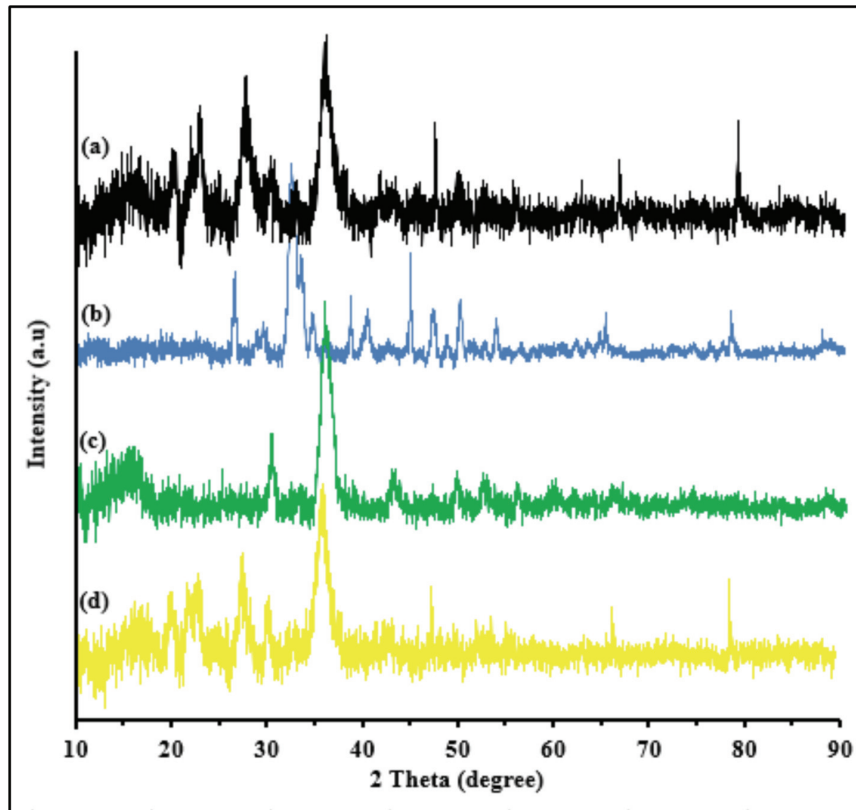


Fig. 4. XRD patterns of (a) CRW, (b) HTC200, (c) PY700, and (d) MW800.

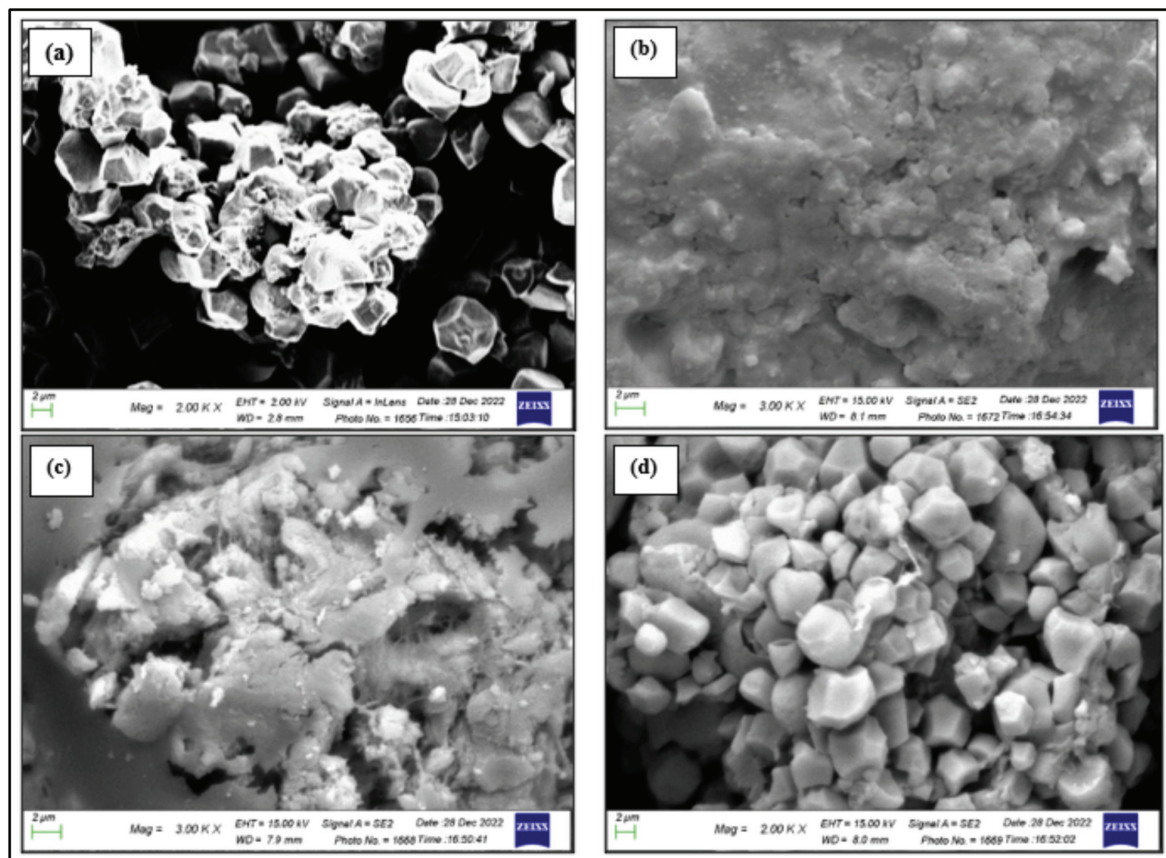


Fig. 5. SEM images of (a) CRW, (b) HTC200, (c) PY700, and (d) MW800.

## 4. Conclusion

The chars were successfully produced by CRW during hydrothermal carbonization, pyrolysis, and microwave irradiation processes. The highest temperature for the production of hydro-char production via HTC process pyrolysis was 200 °C, while the highest temperature of pyro-char production via the pyrolysis process was 700 °C, and the highest microwave power of micro-char production during the microwave process was 800 W. The hydro-char was higher specification than both pyro-char and micro-char, according to a comparison of the physicochemical properties of chars formed by HTC, PY, and MW of CRW under different specified reaction parameters. The chars produced were characterized by using FTIR, XRD, BET, and SEM. As well as recommendations, this study needs to be sustained by doing some descriptions such as high heating value (HHV).

## References

- Economou F, et al. The concept of food waste and food loss prevention and measuring tools. *Waste Manag Res.* 2024;0734242x241237187.
- Dhalsamant K, Tirumareddy P, Borugadda VB, Dalai AK. Utilization of food waste for biocrude production: A review. *Bioresour Technol Reports.* 2023;101595.
- Saba M, et al., Microbial pretreatment of chicken feather and its co-digestion with rice husk and green grocery waste for enhanced biogas production. *Front Microbiol.* 2022;13:792426.
- Zhang L, Ren J, Bai W. A review of poultry waste-to-wealth: Technological progress, modeling and simulation studies, and economic-environmental and social sustainability. *Sustainability.* 2023;15(7):5620.
- Espindola J, Selim OM, Amano RS. Co-pyrolysis of rice husk and chicken manure. *J Energy Resour Technol.* 2021;143(2):22101.
- Syed Hassan SS, et al. Characterization study of petroleum oily sludge produced from north refineries company Baiji to determine the suitability for conversion into solid fuel. *Egypt J Chem.* 2021;0(0):0–0. doi: [10.21608/ejchem.2021.54222.3126](https://doi.org/10.21608/ejchem.2021.54222.3126).
- Dutta S, He M, Xiong X, Tsang DCW. Sustainable management and recycling of food waste anaerobic digestate: A review. *Bioresour Technol.* 2021;341:125915.
- Bao D, Li Z, Liu X, Wan C, Zhang R, Lee D-JJ. Biochar derived from pyrolysis of oily sludge waste: Structural characteristics and electrochemical properties. *J Environ Manage.* 2020;268(2005):110734. doi: [10.1016/j.jenvman.2020.110734](https://doi.org/10.1016/j.jenvman.2020.110734).
- Elkhalifa S, Al-Ansari T, Mackey HR, McKay G. Food waste to biochars through pyrolysis: A review. *Resour Conserv Recycl.* 2019;144:310–320.
- Janu R, et al. Biochar surface functional groups as affected by biomass feedstock, biochar composition and pyrolysis temperature. *Carbon Resour Convers.* 2021;4:36–46.
- Leng L, et al. Nitrogen containing functional groups of biochar: An overview. *Bioresour Technol.* 2020;298:122286.
- Guo M, Song W, Tian J. Biochar-facilitated soil remediation: Mechanisms and efficacy variations. *Front Environ Sci.* 2020;8:521512.
- Barthod J, Rumpel C, Dignac M-F. Composting with additives to improve organic amendments. A review. *Agron Sustain Dev.* 2018;38(2):17.
- Rangabhashiyam S, et al. Sewage sludge-derived biochar for the adsorptive removal of wastewater pollutants: A critical review. *Environ Pollut.* 2022;293:118581.
- Sri Shalini S, Palanivelu K, Ramachandran A, Raghavan V. Biochar from biomass waste as a renewable carbon material for climate change mitigation in reducing greenhouse gas emissions—A review. *Biomass Convers Biorefinery.* 2021;11:2247–2267.
- Xu D, et al. Mini-review on char catalysts for tar reforming during biomass gasification: The importance of char structure. *Energy & Fuels.* 2019;34(2):1219–1229.
- Guo Y, et al. Investigation on co-combustion of coal gasification fine slag residual carbon and sawdust char blends: Physicochemical properties, combustion characteristic and kinetic behavior. *Fuel.* 2021;292:120387.
- Liang M, Zhang K, Lei P, Wang B, Shu CM, Li B. Fuel properties and combustion kinetics of hydrochar derived from co-hydrothermal carbonization of tobacco residues and graphene oxide. *Biomass Convers Biorefinery.* 2020;10(1):189–201. doi: [10.1007/s13399-019-00408-2](https://doi.org/10.1007/s13399-019-00408-2).
- Hasan MM, Rasul MG, Khan MMK, Ashwath N, Jahirul MI. Energy recovery from municipal solid waste using pyrolysis technology: A review on current status and developments. *Renew Sustain Energy Rev.* 2021;145:111073.
- Zhang J, Duan Y, Wang B, Zhang X. Interfacial enhancement for carbon fibre reinforced electron beam cured polymer composite by microwave irradiation. *Polymer (Guildf).* 2020;192:122327.
- Güleç F, Williams O, Kostas ET, Samson A, Lester E. A comprehensive comparative study on the energy application of chars produced from different biomass feedstocks via hydrothermal conversion, pyrolysis, and torrefaction. *Energy Convers Manag.* 2022;270:116260.
- Huang Z, et al. Effects of waste-based pyrolysis as heating source: Meta-analyze of char yield and machine learning analysis. *Fuel.* 2022;318:123578.
- Tripathi M, Bhatnagar A, Mubarak NM, Sahu JN, Ganesan P. RSM optimization of microwave pyrolysis parameters to produce OPS char with high yield and large BET surface area. *Fuel.* 2020;277:118184.
- Fathi MI, Abdulqader MA, Habeeb OA. Microwave process of oily sludge produced at NRC Baiji to micro-char solid carbon production. *Desalin Water Treat.* 2023;310:142–149.
- Ali BM, Salih MI, Abdulqader MA, Bakthavatchalam B, Hussein OA. Dehydration and decarboxylation via pyrolysis process of waste oily sludge accumulated at North Refineries Company Baiji for use as a pyro-fuel. *Desalin Water Treat.* 2024;100330.
- Subramaniam S, Foo KY, Yusof ENM, Jawad AH, Wilson LD, Sabar S. Hydrothermal synthesis of phosphorylated chitosan and its adsorption performance towards Acid Red 88 dye. *Int J Biol Macromol.* 2021;193:1716–1726.
- Jawad AH, Saber SEM, Abdulhameed AS, Farhan AM, ALOthman ZA, Wilson LD. Characterization and applicability of the natural Iraqi bentonite clay for toxic cationic dye removal: Adsorption kinetic and isotherm study. *J King Saud Univ.* 2023;35(4):102630.

28. Jawad AH, Abdulhameed AS. Mesoporous Iraqi red kaolin clay as an efficient adsorbent for methylene blue dye: Adsorption kinetic, isotherm and mechanism study. *Surfaces and Interfaces*. 2020;18:100422.
29. Uddin MK, Abd Malek NN, Jawad AH, Sabar S. Pyrolysis of rubber seed pericarp biomass treated with sulfuric acid for the adsorption of crystal violet and methylene green dyes: An optimized process. *Int J Phytoremediation*. 2023;25(4):393–402.
30. Sing KSW. Reporting physisorption data for gas/solid systems with special reference to the determination of surface area and porosity (Recommendations 1984). *Pure Appl Chem*. 1985;57(4):603–619.
31. Jawad AH, Ismail K, Ishak MAM, Wilson LD. Conversion of Malaysian low-rank coal to mesoporous activated carbon: Structure characterization and adsorption properties. *Chinese J Chem Eng*. 2019;27(7):1716–1727.
32. Zain ZM, Abdulhameed AS, Jawad AH, AlOthman ZA, Yaseen ZM. A pH-sensitive surface of chitosan/sepiolite clay/algae biocomposite for the removal of malachite green and remazol brilliant blue R dyes: Optimization and adsorption mechanism study. *J Polym Environ*. 2023;31(2):501–518.
33. Abd Rashid R, Jawad AH, Azlan M, Ishak M, Kasim NN. FeCl<sub>3</sub>-activated carbon developed from coconut leaves: Characterization and application for methylene blue removal. *Sains Malaysiana*. 2018;47(3):603–610.
34. Ang ZY. Analysis on application of biochar composites in removal of hexavalent chromium from wastewater. UTAR, 2020.
35. Buentello-Montoya D, Zhang X, Li J, Ranade V, Marques S, Geron M. Performance of biochar as a catalyst for tar steam reforming: Effect of the porous structure. *Appl Energy*. 2020;259:114176.